ResearchGate

See discussions, stats, and author profiles for this publication at: https://www.researchgate.net/publication/224213565

Estimation of Induction Motor Operating Power Factor From Measured Current and Manufacturer Data

Article *in* IEEE Transactions on Energy Conversion · July 2011

DOI: 10.1109/TEC.2010.2098408 · Source: IEEE Xplore

CITATIONS
17

READS
1,608

3 authors, including:

Abhisek Ukil
University of Auckland
191 PUBLICATIONS **1,860** CITATIONS

SEE PROFILE

Some of the authors of this publication are also working on these related projects:

Advanced Multi-Sensor Anomaly Monitoring and Analytics for Gas Pipeline View project

DC Grid Protection View project

All content following this page was uploaded by Abhisek Ukil on 19 May 2015.

The user has requested enhancement of the downloaded file.

Estimation of Induction Motor Operating Power Factor From Measured Current and Manufacturer Data

Abhisek Ukil, *Senior Member, IEEE*, Richard Bloch, Andrea Andenna, *Member, IEEE*

***Abstract*— Three-phase induction (asynchronous) motors (IM) are industrial work-horses, making the protection of IM a very important topic. IM protection devices typically monitor the motor current and/or voltage to provide the motor protection functionalities like current overload, over/under voltage, etc. One of the interesting parameters to monitor is the operating power factor (PF) of the IM, which provides better underload protection compared to the motor current-based approaches. Traditionally, PF estimation would require both the voltage and the current measurements in order to apply the displacement method. In this paper, we present a method of determining the operating PF of the IM using only the measured current and the manufacturer data which is typically available from the nameplate and/or datasheet. Experimental results are presented to substantiate the feasibility of the proposed method, validated alongside the state of the art PF estimation methods. Operational PF can be effectively used for underload detection, like in pump application, or PF compensation for improving the power quality.**

***Index Terms*— asynchronous motor, cos phi, current measurement, induction motor, nameplate, pf, power factor compensation, pump protection, reactive power, zero crossing.**

I. Introduction

THREE-phase induction (asynchronous) motors (IM) are industrial work-horses, responsible for consumption of 40 to 50% of generated electrical power [1],[2]. Because of its wide industrial usage, in recent years, there has been lot of focus on IM protection at low and medium voltage levels. Such protection devices typically monitor the motor current and/or voltage to provide the motor protection functionalities like current overload, over/under voltage, etc. One of the interesting parameters to monitor is the operating power factor (PF) (sometimes also referred as $\cos\phi$) of the IM. Traditionally, to monitor the operating PF of the IM, one would require both the voltage and the current measurements, and then apply the displacement method. However, that would require both voltage and current sensors. In this paper, we present a method of determining the operating PF of the IM using only the measured current and the manufacturer data which is typically available from the nameplate and/or datasheet. The method requires no synchronized voltage measurement. Therefore, it can provide a low-cost solution. For detecting low loading conditions, PF is more reliable than the motor current-based approaches as will be described in details later. PF is particularly useful for applications like underload protection of pumps, PF compensation for improving the power quality.

The remainder of the paper is organized as follows. In Section II, background information on the IM equivalent circuit, variation of IM PF with load are explained. Section III explains the current-only method for estimating the operating PF. Experimental setup and the procedures are described in Section IV. Section V presents the comparative results of the PF estimation by the proposed method alongside state of the art methods. Discussions on the results are presented in Section VI, followed by conclusion in Section VII.

Manuscript TEC-00391-2010.R1 revised on November 29, 2010. This work was supported by ABB Corporate Research, Switzerland.

A. Ukil (corresponding author) is with ABB Corporate Research, Segelhofstrasse 1K, Baden-Daettwil, 5405, Switzerland, (phone: +41 58 586 7034, fax: +41 58 586 7358, email: abhisek.ukil@ch.abb.com).

R. Bloch is with ABB Corporate Research, Segelhofstrasse 1K, Baden-Daettwil, 5405, Switzerland, (email: richard.bloch@ch.abb.com).

A. Andenna is with ABB Corporate Research, Segelhofstrasse 1K, Baden-Daettwil, 5405, Switzerland, (email: andrea.andenna@ch.abb.com).

II. Background Information

A. Induction Motor Equivalent Circuit

IM equivalent circuit is an effective method to explain its steady-state operating characteristics [1],[2],[3]. The equivalent circuit of the IM is often analogous to the transformer operation, shown in Fig. 1. The primary and the secondary winding of the transformer can then be assumed to be the stator and the rotor of the IM (see Fig. 2). In Fig. 2, r_1, X_1 stand for the stator resistance and reactance, while r_2, X_2 for the rotor resistance and reactances respectively, s is the slip, (equivalent to the turns ratio of the transformer), V_1 is the supply voltage.

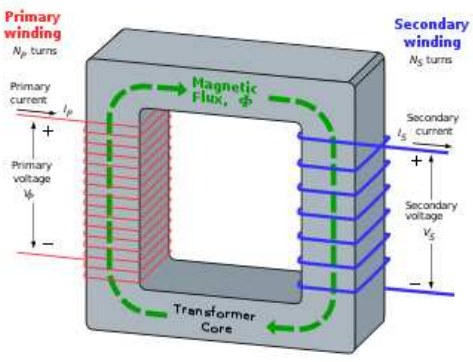

Fig. 1. Transformer operation.

By referring the secondary (rotor) side to the primary (stator), the IM equivalent circuit can be redrawn as in Fig. 3.

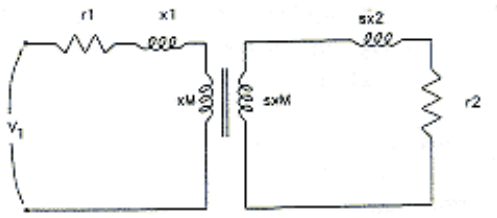

Fig. 2. Induction motor operation analogous to transformer.

From Fig. 3, the stator current I_1 consists of two components. One component I_1' is the load component and counteracts the rotor magnetomotive force (mmf). The other component is the exciting current I_m, whose function is to create the resultant air-gap flux and to provide the core loss. In Fig. 3, r_c and X_m are the core-loss resistance and the magnetizing reactance respectively [1],[2]. The leakage reactances X_1 and X_2' are much smaller than the magnetizing reactance X_m.

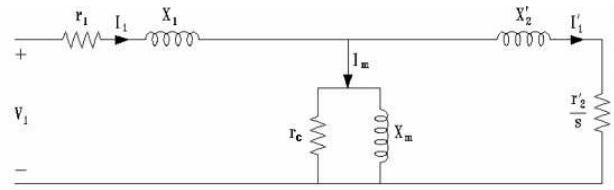

Fig. 3. Induction motor equivalent circuit.

The equivalent circuit parameters can be estimated using the short-circuit and no-load test [3]. Under the no-load test, for example, the slip s is approximately zero, therefore the rotor circuit has an infinite impedance approximately, causing the whole stator current to flow through the magnetizing circuit. Therefore, the no-load test is used to estimate the magnetizing circuit parameters. Nevertheless, from Fig. 3, we see that the reactances, which depend on the IM design, do not change during the IM steady state operation [4], while the rotor resistance changes depending on the motor load.

These parameters are often not given. Many studies present ways to estimate the parameters using measured data and other available information like the manufacturer data [5],[6],[7], etc. Estimation of the operating load of the IM is of importance as reported by Ferreira and colleagues [8]. Pillay and colleagues used motor parameter determination for calculating the transient torque [9]. Among other operational parameters, estimation of the iron losses in IM is reported by Gmyrek and colleagues [10]. Hilairet and colleagues reported flux and velocity estimation of IM using Kalman filters [11].

B. Power Factor & Motor Load

From the equivalent circuit, the vector diagram is drawn for the IM operation, shown in Fig. 4. At no load, the stator current I_0 is shown in Fig. 4. The function of the load component of I_0 at no load is to supply friction and windage loss. As this loss is quite small, the rotor current and therefore the load component is very small. But the magnetizing current forms a major component of the no-load current due to presence of air gap in an IM. As a result, from Fig. 4, the no-load current I_0 lags the stator voltage by an angle θ_0 in the range of 75° to 85° [2]. Consequently, the stator PF at no load may be as low 0.1 to 0.3, the lower values being applicable for larger motors.

As the motor is loaded, the load component of stator current rises above its no-load value, supplying the load torque. Thus, the rotor mmf reacts on the stator and calls for a compensating load component of stator current I_1', such that the stator mmf balances the rotor mmf

$$I_1' N_1 = I_2 N_2, \tag{1}$$

where, N_1 and N_2 are the effective number of turns for the stator and the rotor respectively. Therefore, the stator mmf opposes the equal rotor mmf, as shown in Fig. 4. Accordingly, in Fig. 4, the stator-load component I_1', of the total stator current I_1, is shown as opposite in direction to the rotor current I_2.

The stator-load component I_1' when added to I_0, gives the stator current OA at a PF of $cos\theta_1$ with respect to (w.r.t) V_1'. In Fig. 4, $I_1 r_1$ and $jI_1 X_1$ represent the leakage impedance drop. With further increase of load on the motor, the rotor current increases and the overall stator current is given by OB at a PF of $cos\theta_1'$ w.r.t V_1'. It is thus seen from Fig. 4 that the PF angle decreases, and therefore the stator PF improves as the load on the motor is increased. Typically, stator PF of about 0.8 to 0.9 are obtained at 80 to 100% of the full-load [1],[2].

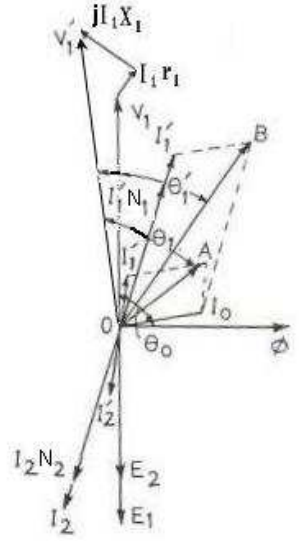

Fig. 4. Vector diagram of induction motor power factor and influence of load.

III. Current-only Power Factor Estimation

The total input electrical apparent power to the motor is given as

$$\hat{P} = \sqrt{3} V I, \tag{2}$$

where V, I are the line voltage and current respectively. The active power, accounting for supplying the load, is given as

$$P = \sqrt{3} V I \cos\phi. \tag{3}$$

The PF is then defined as

$$PF = \frac{P}{\hat{P}} = \cos\phi. \tag{4}$$

As discussed in the previous section, the motor current I would have two components, I_{active} and $I_{reactive}$. Active part of the current (I_{active}) accounts for the torque, changing according to the load (from no-load to full/over-load). Reactive part of the current ($I_{reactive}$) accounts for the magnetizing current of the IM, without changing much from the no-load to the full-load condition, practically remaining constant [1],[2],[4]. This is because for IM, the magnetizing circuit, i.e., the stator coil inductances remain same.

$$I = \sqrt{I_{active}^2 + I_{reactive}^2}, \tag{5}$$

$$I_{active} = I\cos\phi, \tag{6}$$

$$I_{reactive} = I\sin\phi. \tag{7}$$

Utilizing (4) in (7),

$$I_{reactive} = I\sin(\cos^{-1} PF). \tag{8}$$

Eq. (4) can be rewritten as

$$PF = \cos\phi = \sqrt{1-\sin^2\phi} = \sqrt{1-\left(\frac{I_{reactive}}{I}\right)^2}. \tag{9}$$

As the reactive component remains constant, it can be estimated from the nominal condition given by the manufacturer data and/or nameplate data using (8). Now, as the motor load increases, the total motor current (I) in (9) would increase, while $I_{reactive}$ remains constant. Hence, the ratio of ($I_{reactive}/I$) in (9) decreases, causing the PF to increase towards unity. Theoretically, at no-load condition, there is no active current flow. So, at no-load, $I = I_{reactive}$, making the $PF = 0$, theoretically. That is, physically, at no-load, there is not much mechanical resistance, so the whole circuit is mostly inductive due to the stator coils, causing low power factor. Increase in motor load is essentially similar to adding resistances to the circuit, causing the PF to improve.

Therefore, in the current-only PF estimation approach, we would estimate the $I_{reactive}$ using (8) from the nominal PF out of the nameplate data. Then, from the measured motor current and the constant $I_{reactive}$, using (9), we can estimate the operating PF. It would not require synchronized voltage and current measurement like in the displacement PF measurement principle. The displacement PF measurement principle uses the zero-crossing instants and compares the differences between the voltage and the current. It will be shown later in details for comparative analysis of the results using different approaches.

IV. Experiment

For verifying the proposed method, we performed the following experiment. The schematics of the experimental setup is shown in Fig. 5. In Fig. 5, we've a test motor (2.2 kW) [12] supplied from the 50 Hz mains. There is a second motor of slightly bigger size (7.5 kW) [12] directly coupled to the test motor, acting as a loading motor to the test motor. The loading motor is supplied via an ABB drive [13] so that the torque of the loading motor can be changed in order to test different loading conditions for the test motor. In order to load the test motor, the direction of rotation of the loading motor should be opposite to that of the test motor. This can be done via the drive, as indicated in Fig. 5. The test motor is an ABB 3-phase, 2 pole pairs IM, type M2AA LA4 [12]. Fig. 6 shows the nameplate ratings of the test motor. Stator winding of the motor was connected in star (Y). The effective nameplate ratings are given in Table I.

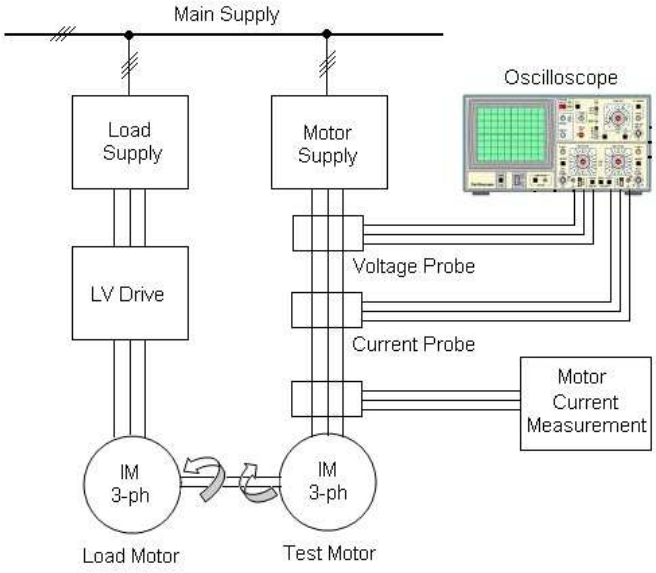

Fig. 5. Experimental setup.

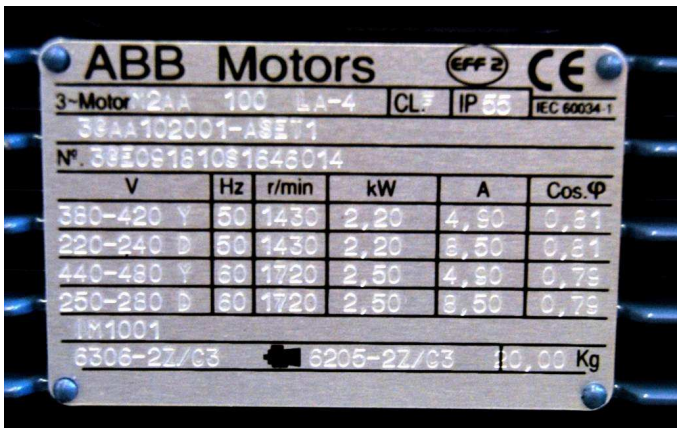

Fig. 6. Nameplate of the test motor.

For the proposed PF measurement, the motor current of the test motor is measured using a motor current measurement module. To validate the proposed current-only PF estimation, the actual PF also needs to be measured. For that purpose, a high-resolution oscilloscope from Agilent [14] is used to make synchronized measurement of the supply voltage and the motor current. The oscilloscope has four input channels. So, two phases of the supply voltage and two phases of the motor currents are measured, synchronized at the scope. For measuring the current, hall-sensor probes [15] are used, while

TABLE I
NAMEPLATE RATING OF THE TEST MOTOR TYPE ABB M2AALA4 CONNECTED IN STAR (Y) FROM 50 HZ SUPPLY

Nominal voltage	400 V
Nominal current	4.9 A
Rated power	2.2 kW
Rated power factor	0.81
Rated speed	1430 RPM

for measuring the supply voltage, high voltage probes from Tektronix [16] are used.

During the experiment, the loading motor torque is controlled via the drive starting from no-load to over-load conditions of the test motor. At each loading condition, the test motor current is measured, along with the synchronized supply voltage and current measurement at the scope. From the voltage and current measurement at scope, also the instantaneous power is measured.

V. APPLICATION RESULTS

A. Power Factor: From Measured Current

From Table I, using (8), we get
$I_{reactive} = 4.9 \sin(\cos^{-1} 0.81) = 2.87$A.

The measured current for the test motor at different loading conditions and the calculated PFs using (9) are shown in Table II. The loading conditions can be specified in terms of % of the rated torque of the load motor (248.48 N.m, 7.5 kW) which is given by the drive. If such load torque measurement from the drive is not present, the loading can be approximated by the motor current as % of the nominal current. The latter is used in this paper and shown in Table II. For example, in the first row of Table II, the measured current is 3.01A, which is $61.43\%(= 3.01/4.9)$ of the nominal current. Using (9), and the $I_{reactive} = 2.87$A for the test motor, we get
$PF = \sqrt{1 - (\frac{2.87}{3.01})^2} = 0.3$.

From the second row, for the measured current of 3.23A which is 65.92% of the nominal current,
$PF = \sqrt{1 - (\frac{2.87}{3.23})^2} = 0.46$.

Value of the rated PF of the test motor is 0.81 (see Table I), which is in between row four and five in Table II for the rated current of 4.9A, as a validation.

TABLE II
MEASURED CURRENT, CALCULATED POWER FACTOR FROM CURRENT ONLY METHOD AT DIFFERENT LOAD

Measured current I (A)	$I/I_{nominal}$ (%)	PF
3.01	61.43	0.30
3.23	65.92	0.46
3.69	75.31	0.63
4.37	89.18	0.75
5.21	106.33	0.83
6.21	126.73	0.89
7.34	149.8	0.92
8.7	177.55	0.94

B. Power Factor: From Voltage, Current Zero-crossing

In the state of the art displacement method of estimating the PF, synchronized measurement of the supply voltage and the motor current are done. Then, the displacements in the zero-crossing (ZC) timings between the voltage (taken as reference) and the current signals are estimated, which would give the PF estimation, i.e., how much the current lags/leads w.r.t the voltage signal.

For example, in the 50 Hz supply, the period of the voltage and current signals would be $1/50$Hz$= 20$ms, which covers 2π rad or $360°$. If there is $\pm x$ ms deviation between the current ZC w.r.t the voltage ZC, then the PF is given as

$$PF = \cos\left(\frac{x}{(1/f_0)} \times 360°\right), \tag{10}$$

where, f_0 is the supply frequency. Whether the current ZC deviation is positive or negative w.r.t the voltage would decide that the PF is lagging or leading. Example of the displacement PF estimation for the experimental setup (see Fig. 5) is shown in Fig. 7 for one phase of the voltage and current.

The synchronized measurement of the supply voltage and the motor current are done in the oscilloscope, Fig. 7 showing the screenshot of the scope. The measurement shown in Fig. 7 corresponds to 66% $I/I_{nominal}$, i.e., for the second row in Table II.

Fig. 7. Power factor measurement using displacement in the zero-crossings of the synchronized supply voltage and motor current at 66% current load.

In Fig. 7, the vertical scale is 100V/division (for voltage), 2A/division (for current). From Fig. 7, the measured peak (positive or negative half) voltage w.r.t the X-axis is 325V and the measured peak (positive or negative half) current w.r.t the X-axis is 4.25A. Therefore, the root mean square (RMS) values of the supply voltage and the motor current are $325/\sqrt{2} = 230$V and $4.25/\sqrt{2} = 3$A respectively.

In Fig. 7, the horizontal scale is given as 5ms/division, i.e., each small division is 1ms. Therefore, from Fig. 7, we get the deviation of the current ZC to be $+3.4$ms. Using (10), we get $PF = \cos(\frac{3.4}{20} \times 360°) = 0.48$.

This is close to the value in the second row, third column in Table II.

Fig. 8 shows another example for an overload condition of 130% $I/I_{nominal}$, close to the sixth row in Table II.

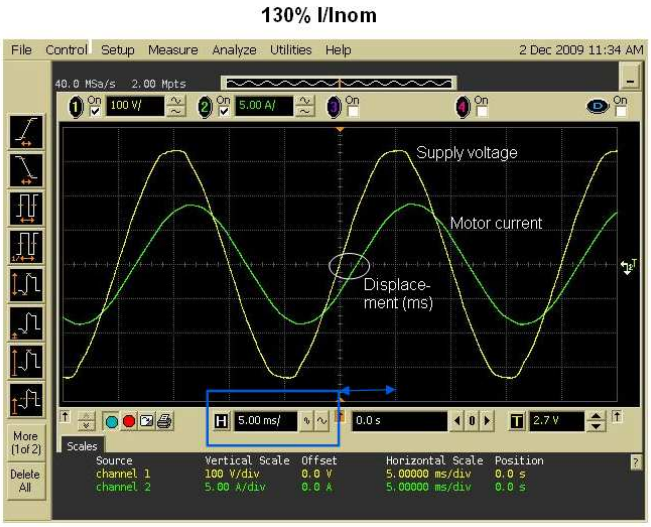

Fig. 8. Power factor measurement using displacement in the zero-crossings of the synchronized supply voltage and the motor current at 130% current load.

In Fig. 8, the vertical scale is 100V/division (for voltage), 5A/division (for current). From Fig. 8, the measured peak (positive or negative half) voltage w.r.t the X-axis is 325V and the measured peak (positive or negative half) current w.r.t the X-axis is 8.75A. Therefore, the RMS values of the supply voltage and the motor current are $325/\sqrt{2} = 230$V and $8.75/\sqrt{2} = 6.19$A respectively. The deviation of the current ZC is $+1.5$ms, giving a PF of 0.89, quite close to the estimated value in the sixth row, third column in Table II.

PFs estimated using the displacement method, utilizing the ZC time differences in (10), at different loading conditions are shown in Table III.

TABLE III

RMS CURRENT, TIME DEVIATION BETWEEN ZC OF VOLTAGE & CURRENT, POWER FACTOR FROM DISPLACEMENT METHOD AT DIFFERENT LOAD

RMS current I (A)	ZC time difference (ms)	PF
2.97	4.6	0.12
3.00	3.4	0.48
3.54	2.8	0.64
4.24	2.1	0.79
5.23	1.6	0.87
6.19	1.5	0.89
7.42	1.4	0.90
8.84	1.3	0.92

C. Power Factor: From Instantaneous Power

In addition to the ZC time displacement method, we also calculated the PF via the instantaneous power (P) measurement method utilizing the synchronized supply voltage (V) and the motor current (I) measurements in the oscilloscope. In this method, from the synchronized supply voltage and the motor current waveforms, we calculate the instantaneous power per phase (i.e., point by point multiplication of the two waveforms). We utilized the average power ($\bar{P}$) per phase from the measurement in the scope. Then by this method, the PF is given as

$$PF = \frac{\bar{P}}{VI}. \tag{11}$$

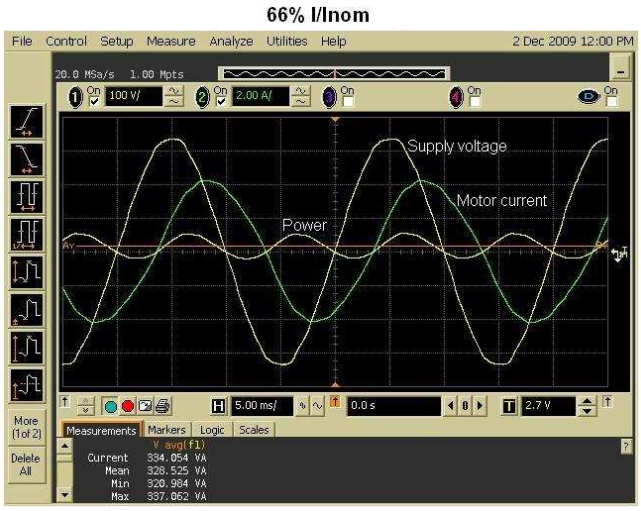

Fig. 9. Power factor measurement using instantaneous power from the measured synchronized supply voltage and the motor current at 66% current load.

Example of the PF estimation from the instantaneous power measurement for the experimental setup (see Fig. 5) at 66% current loading is shown in Fig. 9.

The RMS values of the supply voltage and the motor current for this loading are 230V and 3A respectively. From Fig. 9, the average instantaneous power, $\bar{P} = 328.525$W. Using (11), we get

$PF = \frac{328.525}{230\times 3} = 0.476.$

This is very well matching with the values in the second row of Tables II & III.

PF estimation from the instantaneous power measurement for the overload condition of 130% current loading is shown in Fig. 10. The RMS values of the supply voltage and the motor current for this loading are 230V and 6.19A respectively. From Fig. 10, the average instantaneous power, $\bar{P} = 1.273$kW. Using (11), we get

$PF = \frac{1273}{230\times 6.19} = 0.89.$

This is similar to the values in the sixth row of Tables II & III.

PFs estimated using the instantaneous power method, at different loading conditions are shown in Table IV.

VI. DISCUSSION OF RESULTS

1) Comparison of the PFs at different loads estimated using the proposed current-only method (Table II), state of the art ZC time displacement method (Table III), and the instantaneous power method (Table IV) reveals

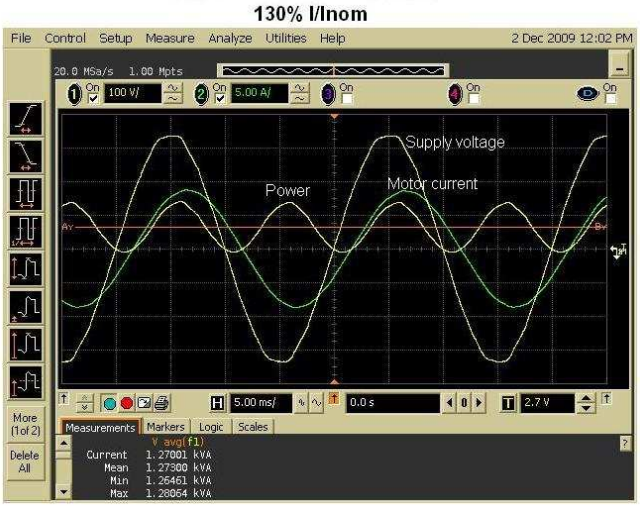

Fig. 10. Power factor measurement using instantaneous power from the measured synchronized supply voltage and the motor current at 130% current load.

TABLE IV
RMS CURRENT, RMS VOLTAGE, INSTANTANEOUS POWER, POWER FACTOR AT DIFFERENT LOAD

RMS current (A)	RMS voltage (V)	Instantaneous power (W)	PF
2.97	230	72.86	0.11
3.00	230	328.53	0.48
3.54	230	547.38	0.67
4.24	230	774.67	0.79
5.23	230	1014.32	0.84
6.19	230	1273.0	0.89
7.42	230	1548.59	0.91
8.84	230	1857.11	0.91

good performance of the current-only method against the voltage and current measurement-based methods using a high-resolution oscilloscope. The PF estimation error using the current-only method is about $+0.04$, except at the no-load condition, where it is about -0.18. This could be because, the sensitivity of the motor current measurement module might not be very perfect at no-load condition.

2) The proposed method relies on the fact that the inductance of the total circuit remains constant. This is true when there are no other inductive and/or capacitive elements other than the IM itself present between the motor and the current measurement. In our experiment, this is maintained as the test motor is directly connected to the supply with no other inductive and/or capacitive elements between its current measurement (see Fig. 5). This rule might be violated if the motor is supplied via a variable speed drive. However, most modern drive systems usually measure both voltage, current and provide/could provide PF measurement [4],[13]. Hence, there would be no need for cheaper calculation of PF. In comparison, the proposed method is aimed at applications where no drives or similar devices of higher cost are available. So, this constraint can be expectedly fulfilled, providing the intended benefit of the proposed method.
3) The current-only method would require no voltage sensors. It would only require the measured motor current (see Table II). However, to estimate the reactive current, it would require the nominal or rated values from the nameplate and/or motor datasheet. As the method relies heavily on the rated values from the nameplate data, the reliability of such nameplate values would be of importance. Quality of the nameplate data might vary from manufacturer to manufacturer, affecting the accuracy of the PF estimation. However, it is expected that manufacturers comply with the relevant IM manufacturing standards, providing rated values with acceptable accuracy. As the results of the proposed method match very closely to the state of the art methods in this work, the nameplate data of the motors [12] used in the tests seem very reliable.
4) In this work, relatively smaller size IMs are used. For bigger IMs with low I_{noload}/I_{rated} ratio, the assumption to use $I_{reactive} = constant$ for light loads might lead to high errors in the PF estimation. This would need to be verified in future works for higher power machines using the proposed method. However, higher power machines are in general more costly, and do not typically employ low-end controllers. Higher power machines usually come with MV or LV drives [13] (depending on the voltage levels), which already provide the PF computation. Therefore, from the practical point of view, there would not be much need for cheaper computation of the PF for bigger machines, as proposed in this work. Instead, the proposed approach would be attractive for the commonly used IMs with typical power rating as in this work, where often low-cost motor controllers are used.
5) From Fig. 3, under no-load condition, the rotor circuit would have approximately infinite impedance. Hence, at no-load condition, the referred reactance of the rotor X_2' would be absent. The no-load current would comprise of the magnetizing current only. Therefore, the no-load current would not be a good representative of the total reactive current. In comparison, the nameplate data gives rated condition, which takes into consideration the whole circuit shown in Fig. 3. So, the reactive current estimated from the rated condition, as proposed in this paper, would not miss any inductive elements, which is very essential for the proposed method.
6) Fig. 11 shows the underload protection schemes using the motor current in plot (i), and the PF in plot (ii). The motor load (as % of measured/nominal current) is plotted along the X-axis. From Fig. 11, the motor current in general provides good overview of the motor load. However, at low loads (e.g., between 60-80% of the current load), the nonlinear curve of the PF provides better resolution than the motor current for small change of load. It is also very challenging to accurately measure the low current change from small

load change at low loading due to effects like saturation, etc. Therefore, the PF is more reliable in such situations. For example, in the pump applications [17],[18],[19], underload protection is important in order to prevent dry running of the pump.

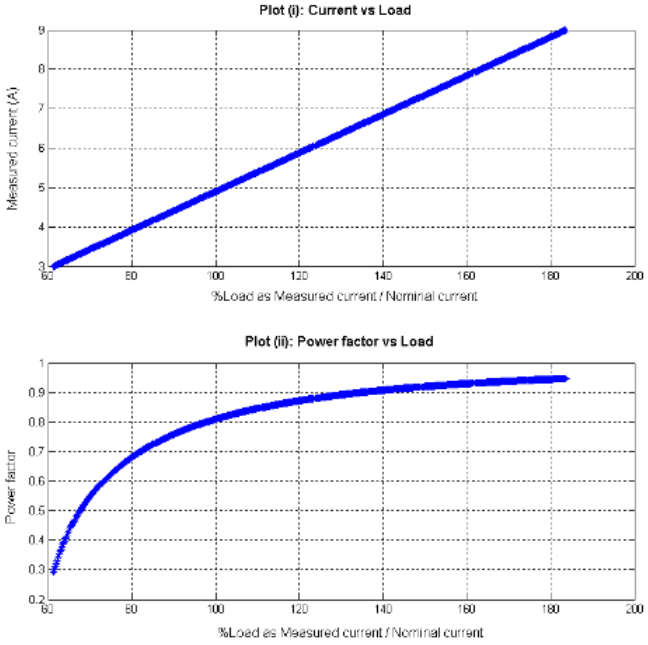

Fig. 11. Underload protection using motor current (plot i), power factor (plot ii).

7) Estimation of IM operating PF could be used for PF compensation [20],[21],[22]. PF compensation is an effective technique to improve the power quality [23],[24]. PF compensation for IM is particularly important because IM is one of the common sources for PF degradation due to its widespread usage across various industries.
8) For the PF estimation using the supply voltage and the motor current ZC displacement method, it is required to match the correct voltage and current phase. This has been done in the following way. At a certain loading condition, we fix the supply voltage probe. Then, the current probe is altered for the three-phases (as it is a 3-phase supply), and three sets of voltage and current measurements are obtained. Out of the three phases, one would be in phase with the voltage (with 0° difference), other two phases of the current would vary by $\pm 120^\circ$, i.e., in terms of ZC displacement, $(\frac{20\times 120^\circ}{360^\circ} =) \pm 6.67$ ms. For example, at 66% $I/I_{nominal}$ load, the voltage and the current for say, phase 1 are shown in Fig. 7, from which, we get the ZC displacement of $+3.4$ms. Keeping the voltage probe fixed, measurements of the current signal from the two other phases (say phase 2 & 3) are shown in Figs. 12 & 13. From Fig. 12, the ZC displacement (indicated by the oval box) is $+10$ms $(= 3.4 + 6.67)$ms, while from Fig. 13, the ZC displacement is -3.3ms $(= 3.4 - 6.67)$ms. Therefore, the matching voltage and current phases correspond to the ones shown in Fig. 7. Once we know the matching phases, those will be fixed for all loads, so can be marked and used.
9) For the PF estimation using the instantaneous method, it is required to match the correct voltage and current phase. It can follow from the matching procedure for the displacement method. Otherwise, it can be done in the following way. At each loading conditions, the supply voltage probe should be fixed, and then the current probe should be altered for the three-phases. The power should follow the load change. That is, if the load is increased or decreased, the power should increase or decrease accordingly. For a mismatched voltage and current phase, this would not be the case. That is, one would observe the power decreases while load is increased, or vice versa.

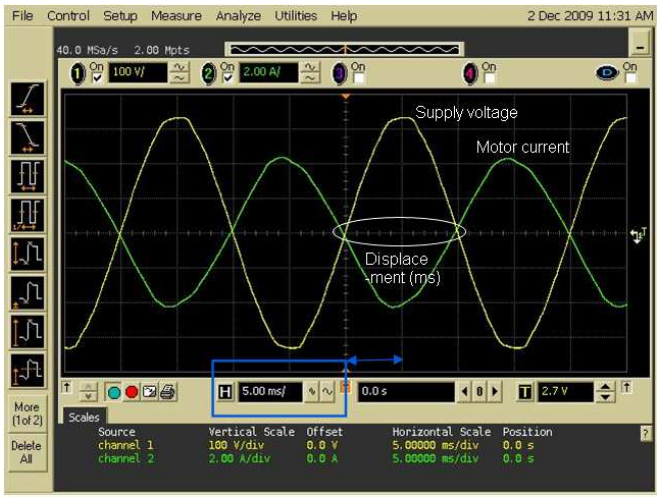

Fig. 12. Power factor measurement using displacement in the zero-crossings of the synchronized voltage and current (phase 2) signals at 66% current load.

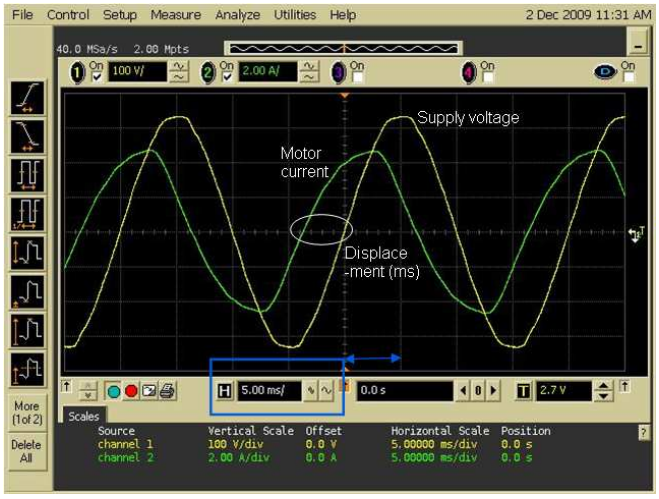

Fig. 13. Power factor measurement using displacement in the zero-crossings of the synchronized voltage and current (phase 3) signals at 66% current load.

View publication stats

VII. Conclusion

For the IM, the operating power factor is one of the interesting parameters to monitor, which provides better underload protection compared to motor current based approaches. Traditionally, PF estimation would require both the voltage and the current measurement in order to apply the zero crossing displacement method. In this paper, we presented a method of determining the operating PF of the IM using only the measured current and the manufacturer data typically available from the nameplate and/or datasheet. From the rated conditions (from the nameplate data), the reactive component of the motor current is estimated, which remains constant for different loading conditions, as per the IM principle [1],[2]. Then, using the measured total motor current and the estimated constant reactive part, the PF can be estimated at different loads. Experimental results are shown using a realistic test setup. PF is estimated using the proposed method, alongside the state of the art voltage & current ZC displacement method and the instantaneous power method measured using a high resolution oscilloscope and synchronized measurements of the supply voltage and the motor current. The accuracy of the proposed method is very promising when compared to the state of the art methods for the class (power rating, pole pairs, etc) of motor used. This would provide a cheaper solution to underload protection, e.g., in pump applications, using the operating PF, without requiring the voltage sensors. Operational PF can also be used for PF compensation for improving the power quality.

Acknowledgments

The authors would like to thank the anonymous reviewers for the constructive review, helping to upgrade the paper.

References

[1] M. G. Say, *Alternating Current Machines*, John Wiley, New York, 1984.
[2] P. S. Bimbhra, *Electrical Machinery*, Khanna Publ., New Delhi, 1997.
[3] A. Gastli, "Identification of induction motor equivalent circuit parameters using the single-phase test," *IEEE Trans. Energy Conversion*, vol. 14, no. 1, pp. 51–56, 1999.
[4] D. Finney, *Variable frequency AC motor drive systems*, Peter Peregrinus Ltd, London, 1991.
[5] J. Pedra, "On the Determination of Induction Motor Parameters From Manufacturer Data for Electromagnetic Transient Programs," *IEEE Trans. Power Systems*, vol. 23, no. 4, pp. 1709–1718, 2008.
[6] M. H. Haque, "Determination of NEMA Design Induction Motor Parameters From Manufacturer Data," *IEEE Trans. Energy Conversion*, vol. 23, no. 4, pp. 997–1004, 2008.
[7] T. Phumiphak, C. Chat-uthai, "Estimation of induction motor parameters based on field test coupled with genetic algorithm," IEEE Int. Conf. Power Syst. Tech. PowerCon, pp. 1199–1203, 2002.
[8] F. Ferreira, A. de Almeida, "Considerations on In-Field Induction Motor Load Estimation Methods," IEEE Int. Conf. Electrical Machines, 2008.
[9] P. Pillay, R. Nolan, T. Haque, "Application of genetic algorithms to motor parameter determination for transient torque calculations," *IEEE Trans. Industrial Applications*, vol. 33, no. 5, pp. 1273–1282, 1997.
[10] Z. Gmyrek, A. Boglietti, A. Cavagnino, "Estimation of Iron Losses in Induction Motors: Calculation Method, Results, and Analysis," *IEEE Trans. Industrial Electronics*, vol. 57, no. 1, pp. 161–171, 2010.
[11] M. Hilairet, F. Auger, C. Darengosse, "Two efficient Kalman filters for flux and velocity estimation of induction motors," IEEE Int. Power Electronics Specialists Conf., PESC, pp. 891–896, 2000.
[12] ABB, "Manual for Low Voltage Motor," 2009. Available: http://www.abb.com/motors
[13] ABB, "LV Drives, model ACS800," 2010. Available: http://www.abb.com/drives
[14] Agilent, "Datasheet Oscilloscope, model Infiniium 54832D." Available: http://www.home.agilent.com/agilent/product.jspx?pn=54832D
[15] Tektronix, "Current Probe Amplifier, model TM503B."
[16] Tektronix, "High Voltage Probe, model P6009."
[17] T. Ahonen, et. al., "Pump Operation Monitoring Applying Frequency Converter," IEEE Symp. Power Electronics SPEEDAM, 2008.
[18] P. G. Kini, R. C. Bansal, "Effect of Voltage and Load Variations on Efficiencies of a Motor-Pump System," *IEEE Trans. Energy Conversion*, vol. 25, no. 2, pp. 287–292, 2010.
[19] D. A. Jarc, D. P. Connors, "Variable Frequency Drives and Power Factor," *IEEE Trans. Ind. Appl.*, vol. IA-21, no. 4, pp. 771–777, 1985.
[20] L. Yun Wei, M. Pande, N. Zargari, W. Bin, "An Input Power Factor Control Strategy for High-Power Current-Source Induction Motor Drive With Active Front-End," *IEEE Trans. Power Electronics*, vol. 25, no. 2, pp. 352–359, 2010.
[21] L. Yun Wei, M. Pande, N. Zargari, W. Bin, "Power-Factor Compensation for PWM CSRCSI-Fed High-Power Drive System Using Flux Adjustment," *IEEE Tr. Power Electronics*, vol. 24, no. 12, pp. 3014–3019, 2009.
[22] A. Cavallini, G. Mazzanti, G. C. Montanari, C. Romagnoli, "Design of shunt capacitor circuits for power factor compensation in electrical systems supplying nonlinear loads: a probabilistic approach," *IEEE Trans. Industry Applications*, vol. 34, no. 4, pp. 675–681, 1998.
[23] D. Sharon, "Power factor definitions and power transfer quality in nonsinusoidal situations," *IEEE Trans. Instrumentation and Measurement*, vol. 45, no. 3, pp. 728–733, 1996.
[24] E. Garcia-Canseco, R. Grino, R. Ortega, M. Salichs, A. M. Stankovic, "Power-factor compensation of electrical circuits," *IEEE Control Systems Magazine*, vol. 27, no. 2, pp. 46–59, 2007.

Abhisek Ukil (S'05-M'06–SM'10) received the bachelors degree in electrical engineering from the Jadavpur Univ., Calcutta, India, in 2000 and the M.Sc. degree in electronic systems and engineering management from the Univ. of Bolton, Bolton, UK in 2004. He received his Ph.D. from the Tshwane Univ. of Technology, Pretoria, South Africa in 2006.

After joining in 2006, currently he is a Principal Scientist at 'Integrated Sensor Systems' group, ABB Corporate Research, Baden-Daettwil, Switzerland. He is author/coauthor of more than 40 published scientific papers including a monograph *Intelligent Systems and Signal Processing in Power Engineering* (Springer, Heidelberg, 2007), inventor/co-inventor of 6 patents. His research interests include signal processing, machine learning, power systems and embedded systems.

Richard Bloch received the diploma in electrical engineering from the ABB professional college, Baden, Switzerland in 1974. Since 1974, he has developed measurement systems for different internal ABB companies. After joining in 1989 at the ABB Corporate Research, Baden-Daettwil, Switzerland, currently he is a Technical Expert at 'Integrated Sensor Systems' group. His current research interests include measurement technique, development of EMC-proof analog, digital and low power circuit.

Andrea Andenna (M'02) received his M.Sc. engineering degree in industrial automation and control systems from the Technical University of Milan (Politecnico di Milano), Milan, Italy in 1998. Currently, he is the responsible of the 'Integrated Sensor Systems' group of the ABB Corporate Research, Baden-Daettwil, Switzerland. The group focuses on electronics and signal processing for field devices, analytical instruments and sensors in general. He is author of over 20 publications and patents in the industrial automation and sensors area.